

Programmable Laser-Assisted Surface Microfabrication on a Poly(Vinyl Alcohol)-Coated Glass Chip with Self-Changing Cell Adhesivity for Heterotypic Cell Patterning

Yi-Chen Li,^{†,‡} Meng-Wei Lin,^{†,‡} Meng-Hua Yen,^{†,‡} Sabrina Mai-Yi Fan,[†] June-Tai Wu,[§] Tai-Horng Young,[†] Ji-Yen Cheng,[‡] and Sung-Jan Lin^{*,†,||,⊥,¶}

[†]Institute of Biomedical Engineering, College of Medicine and College of Engineering, National Taiwan University, No. 1, Section 1, Jen-Ai Road, Taipei 100, Taiwan

[‡]Research Center for Applied Sciences, Academia Sinica, Taipei 115-29, Taiwan

[§]Institute of Molecular Medicine, College of Medicine, National Taiwan University, Taipei 100, Taiwan

^{||}Department of Dermatology, National Taiwan University Hospital and College of Medicine, Taipei 100, Taiwan

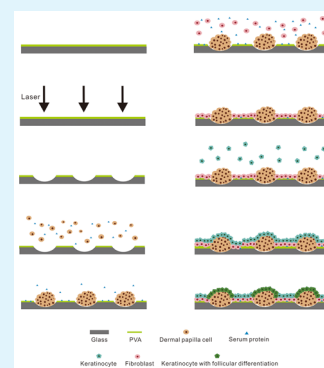
[⊥]Research Center for Developmental Biology and Regenerative Medicine, National Taiwan University, Taipei 100, Taiwan

[¶]Molecular Imaging Center, National Taiwan University, Taipei 100, Taiwan

S Supporting Information

ABSTRACT: Organs are composed of heterotypic cells with patterned architecture that enables intercellular interaction to perform specific functions. In tissue engineering, the ability to pattern heterotypic cells into desired arrangement will allow us to model complex tissues in vitro and to create tissue equivalents for regeneration. This study was aimed at developing a method for fast heterotypic cell patterning with controllable topological manipulation on a glass chip. We found that poly(vinyl alcohol)-coated glass showed a biphasic change in adhesivity to cells in vitro: low adhesivity in the first 24 h and higher adhesivity at later hours due to increased serum protein adsorption. Combining programmable CO₂ laser ablation to remove poly(vinyl alcohol) and glass, we were able to create arrays of adhesive microwells of adjustable patterns. We tested whether controllable patterns of epithelial-mesenchymal interaction could be created. When skin dermal papilla cells and fibroblasts were seeded respectively 24 h apart, we were able to pattern these two cells into aggregates of dermal papilla cells in arrays of microwells in a background of fibroblasts. Seeded later, keratinocytes attached to these mesenchymal cells. Keratinocytes contacting dermal papilla cells started to differentiate toward a hair follicle fate, demonstrating patternable epithelial-mesenchymal interaction. This method allows fast adjustable heterotypic cell patterning and surface topology control and can be applied to the investigation of heterotypic cellular interaction and creation of tissue equivalent in vitro.

KEYWORDS: surface topology, tissue equivalent, hair follicle, dermal papilla, keratinocyte, fibroblast



INTRODUCTION

Spatial organization of heterotypic cells affects cellular interaction and is vital to organ development and function.^{1–3} Cellular interaction is a dynamic process that can be mediated by both long-range cytokine/morphogen secretion and short-range intercellular contact.^{2,4–7} Hence, arrangement and even alignment of cells in space can affect cellular functions because of the corresponding changes of spatial cytokine/morphogen gradient profile as well as extent and character of intercellular contact. To model cellular interaction in vitro and to create tissue equivalent for tissue regeneration, methods for quick patterning of heterotypic cells into desired topological arrangement are of high significance in terms of both experimental testing and potential clinical application.

To understand heterotypic cellular interaction, cells of different types should be cocultured. A transwell system is often employed to examine how heterotypic cells interact with paracrine secretion.^{8,9} In this system, two types of cells are cultured together but separated by a porous membrane across which movement of proteins and small

molecules but not cells is allowed.^{8,9} Since heterotypic cells are separated, the role of heterotypic cell–cell contact can not be analyzed. Another conventional method to examine heterotypic cellular interaction is to culture two different types of cells in a conventional culture dish by simultaneous heterotypic cell seeding.¹⁰ Though contact between heterotypic cells are allowed, the spatial distribution of cells can not be controlled to mimic the in vivo heterotypic cell distribution, prohibiting further analysis of the effect of patterns of heterotypic cell–cell contact.

With the advent of tissue engineering, a number of in vitro techniques have been developed to simulate the in vivo intercellular arrangement for analysis of cellular interaction. Examples include photolithography, soft lithography (including stencil-assisted patterning, microcontact printing and microfluidic patterning), bioprinting,

Received: July 3, 2015

Accepted: September 22, 2015

Published: September 22, 2015

etc.^{11–18} These techniques mainly create patternable domains of varied cell adhesivity on culture surface. In bioprinting, cells can be directly printed to the culture surface with desired distribution.^{17,18} For example, using photolithography to pattern adhesive biomolecules on glass surface has helped to culture hepatocytes and fibroblasts into patterned distribution to dissect the role of homotypic and heterotypic cell–cell contact in the maintenance of hepatocyte functions.^{7,12} Though these methods help to examine cell–cell interaction and create complex tissue-like structures in vitro, there exist limitations such as complex manufacturing procedures, limited patternable flexibility, vulnerability of patterning equipment, etc.

Here, we developed a method combining surface biomaterial coating and laser microfabrication that allows fast and adjustable heterotypic cell patterning. Over the past few years, laser has been employed in surface microfabrication for biomedical application. Since the beam property and irradiation of laser can be programmably controlled, the surface topology is refabricated and redesigned with ease, reducing the overall duration from testing to manufacture from days to hours.^{19,20} Such advantageous fabrication profiles are difficult to achieve via standard photolithography and soft lithography process.^{19,21} Laser systems, such as nanosecond/ultrafast femtosecond laser,^{22,23} can be used in high-quality machining to produce crack-free and debris-free surface. However, they are not widely available due to the relatively high cost. CO₂ laser is a more economical system with high fabrication flexibility and has been demonstrated to be capable of creating complex structures on plastics or glass surfaces.^{19,24}

The adhesion, migration, proliferation, differentiation, and aggregation of cells can be regulated by the coated materials.^{25–29} If a nonadhesive material is coated on an adhesive surface as a barrier, cells do not attach.³⁰ Patterned removal of the nonadhesive material will allow cells to adhere into patterns with the material removed. For heterotypic cell patterning, a later seeded second cell type will not be able to attach to the surface where the coated material still remains. We speculate that if the coated material shows a time-dependent increase in cell adhesivity, the later seeded second cell type will be able to attach to the surface where the coated material is present, enabling heterotypic cell patterning. We found poly(vinyl alcohol) (PVA) exhibits this unique property. We employed CO₂ laser for surface microfabrication on PVA-coated glass chip. We demonstrated that this method is capable of patterning heterotypic cells of hair follicle dermal papilla (DP) cells, skin fibroblasts, and keratinocytes into desired patterns for controllable epithelial–mesenchymal interaction.

■ EXPERIMENTAL SECTION

Poly(Vinyl Alcohol) (PVA) Preparation and Surface Microfabrication by CO₂ Laser Ablation. A 2.5% (w/w) solution of poly(vinyl alcohol) (PVA) (Chemica Fluka, M.W. = 72 000 g/mol, Switzerland) was prepared by dissolving in dimethyl sulfoxide (DMSO) (Merck, Germany) as we previously described.³⁰ For preparing PVA-coated glass, 80 μ L of PVA solution was coated on a glass chip (20 mm \times 20 mm, thickness = 1.1 mm, Kenteh Optical Co., Ltd., Taiwan). The solution was then allowed to dry in the oven at 60 $^{\circ}$ C. Further surface microfabrication was achieved by use of a modified commercial CO₂ laser scribe (M-300, Universal Laser Systems, U.S.A.) as we previously described.¹⁹ The patterns were designed with commercial computer software and then transferred to the laser scribe for ablation. During scribing, the laser beam was scanned using a CNC-driven stage. The maximum laser power was 0.75W and the beam scanning speed was programmable over the range of 0.6–600 mm s⁻¹. The diameters of 150 and 200 μ m for ablated area size (ψ) and the edge-to-edge distance (D) of 150, 200, 450, and 750 μ m were tested. The unirradiated glass was used as control.

Cell Isolation, Expansion, and Culture Medium. The experimental protocol involving animals was approved by our Institutional Animal Care and Use Committee. DP cells were

isolated and expanded from vibrissae of 6-week-old Wistar rats as we previously described.²⁹ DP cells at passage 3 were used in the following experiments. Fibroblasts were isolated and expanded from cheeks of Wistar rats. Briefly, dermal tissue fragments were first digested in 2 mg/mL collagenase I (Sigma-Aldrich, U.S.A.) in DMEM (Invitrogen, Carlsbad, CA, U.S.A.) at 37 $^{\circ}$ C for 1.5 h, and then fibroblasts from dermal tissue were cultured in culture medium DMEM/F-12 (1:1, Invitrogen, Carlsbad, CA, U.S.A.) with 20% fetal bovine serum (FBS) (Biological Industries, U.S.A.) and 1% antibiotic-antimycotic liquid (Invitrogen, Carlsbad, CA, USA) for 2 days. Afterward, culture medium of DMEM/F-12 with 10% fetal bovine serum was replaced every 3 days. Cells at passage 2 were used in the following experiments. Keratinocytes were isolated from the foot pads of Wistar rats as described.²⁸ The skin of hind foot pads was removed and immersed in 5 U/mL Dispase solution (Gibco, U.S.A.) at 37 $^{\circ}$ C for 1.5 to 2 h. The epidermis was then separated from the dermis and immersed in 0.1% trypsin at 37 $^{\circ}$ C for 1 h. The keratinocytes were isolated and the cell suspension was filtrated through a 40 μ m cell strainer (BD Biosciences, U.S.A.), leaving the keratinocytes in the suspension. Culture medium in the coculture experiments was a 1:1:1 mixture of DMEM, DMEM/F-12 and K-SFM (Invitrogen, Carlsbad, CA, U.S.A.) containing 6.7% FBS, bovine pituitary extract (BPE) (16.7 μ g/mL), recombinant epidermal growth factor (rEGF) (1.67 ng/mL) and 1% antibiotic-antimycotic liquid.

Cell Seeding and Cell-Substratum Adhesivity. The methods were described in our previous work.²⁸ For determining the effect of seeding cell density on DP microtissue formation, cell densities were serially doubled from 2.5×10^4 /cm² to 1.0×10^5 /cm². For patterning of the three heterotypic cell types, DP cells were seeded at the density of 1.0×10^5 /cm², fibroblasts were seeded at the density of 5×10^4 /cm² and keratinocytes were seeded at the density of 1.0×10^5 /cm². Cell–substratum adhesivity was determined by cell numbers attached to the substratum 6 h after seeding of 5×10^4 /cm² DP cells, fibroblasts or keratinocytes on PVA-coated glass or uncoated glass.

Identification of PVA, Changes in Cell–Substratum Adhesivity and Quantification of Serum Protein Adsorption. To characterize the surface with PVA-coating, the surface chemical composition was analyzed by attenuated total reflection (ATR)/Fourier transform infrared (FTIR) spectroscopy by a Nicolet Impact 410 spectrophotometer provided with an ATR device.³¹

To determine the time-dependent changes in cell-substratum adhesivity of PVA-coating, PVA-coated glass was immersed in DMEM containing 10% FBS for 0, 1, 2, 3, and 4 days respectively and then washed with PBS. The adhesivity to fibroblasts and dermal papilla was then determined by the number of cells attached at 6 h after cell seeding. Uncoated glass was used as control.

For quantification of adsorbed serum protein, uncoated and PVA-coated glass were immersed in DMEM containing 10% FBS for 0, 1, 2, 3, and 4 days respectively and then washed with PBS. Bicinchoninic acid protein assay kit (Sigma-Aldrich) was employed to quantify adsorbed serum protein by an ELISA plate reader (SpectraMax M2e, Molecular Devices) according to the instruction of the supplier.

Character of Heterotypic Cell Patterns. To characterize the cell distribution patterns, a confocal microscope (Meta510, Carl Zeiss, Germany) was employed to analyze the 3-

dimensional distribution of cells on the glass chip. DP cells, fibroblasts, and keratinocytes were labeled with red (10 $\mu\text{M}/\text{mL}$, CellTracker Orange CMRA, Invitrogen, U.S.A.), green fluorescent cell tracers (10 $\mu\text{M}/\text{mL}$, CellTracker Green CMFDA, Invitrogen, U.S.A.) and Hoechst (5 $\mu\text{g}/\text{mL}$, Hoechst 33345, Invitrogen, U.S.A.) respectively for 45 min at 37 $^{\circ}\text{C}$ before cell seeding.

Scanning electron microscopic examination was performed as we previously described.³² Briefly, the specimen was washed with PBS and then fixed in 2.5% paraformaldehyde for 20 min and 1% osmium tetroxide (OsO_4) for 1 h, followed by serial dehydration by graded ethanol changes. The specimens were then gold sputtered in vacuum and examined with a scanning electron microscope (SEM) (Field Emission Scanning Electron Microscope, JEOL JSM-6700F).

To characterize cell differentiation with immunostaining, the specimens were fixed in 4% paraformaldehyde at 4 $^{\circ}\text{C}$ for 20 min, perforated with 1% triton-X 100 (Sigma-Aldrich) for 5 min and blocked with 10% bovine serum albumin (Sigma-Aldrich) for 10 min. The primary antibodies included fibronectin (Thermo Fisher Scientific, UK) and keratin 6 (Santa Cruz Biotechnology, U.S.A.) and secondary antibodies included rhodamin-conjugated antimouse IgG antibody (Chemicon, Millipore, U.S.A.) and FITC-conjugated anti goat IgG (Abcam, U.S.A.). The specimens were visualized under a fluorescent microscope (Lieca DMI600, Germany). The activity of alkaline phosphatase was determined as we previously described²⁹

Statistical Analysis. Data were expressed as mean \pm standard error of the mean. Student's *t* test was performed for comparison. *p*-values were considered significant when less than 0.05.

RESULTS

Characterization of PVA Coating. After PVA coating, we analyzed the PVA-coated surfaces by ATR-FTIR. Compared with uncoated glass showing the peak at 1000 cm^{-1} (Si-O-Si) (Figure 1), PVA-coated glass chip showed alcohol peak and alkyl peak at 3300 cm^{-1} (-OH), 2850–2950 cm^{-1} (-CH), 1750 cm^{-1} (-CH₂), and 1250 cm^{-1} (C-O). This result demonstrated that the glass surface was covered by coated PVA.

Cell-Substratum Adhesivity. We compared the cell-substratum adhesivity of DP cells, fibroblasts, and keratinocytes

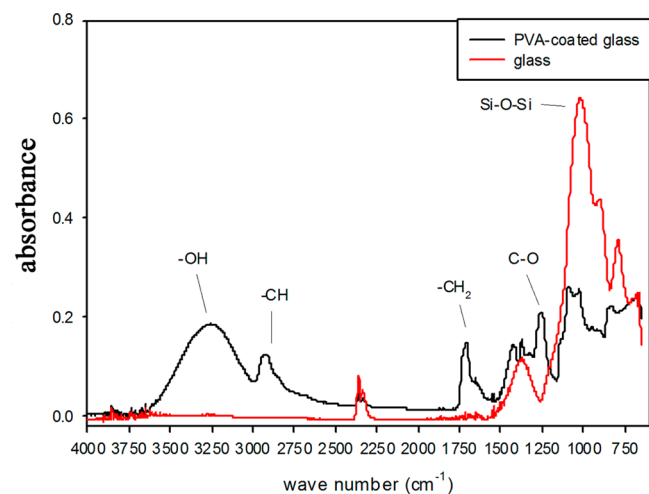


Figure 1. ATR/FT-IR spectra of the glass and PVA-coated glass.

on uncoated glass and PVA-coated glass (Figure 2). We observed that glass was highly adherent to DP cells and

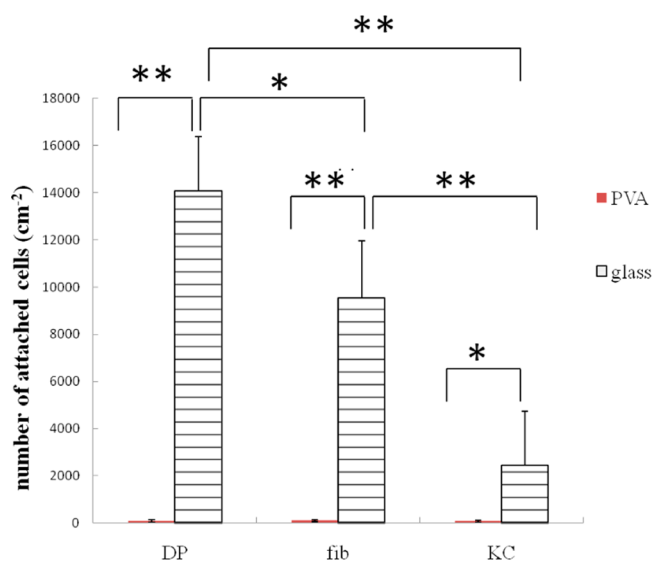


Figure 2. Cell substratum adhesivity determined by cell numbers attached to culture surface at 6 h after cell seeding. The adhesivity of PVA and glass to DP cells, fibroblasts (fib), and keratinocytes (KC) was determined. **p* < 0.05, ***p* < 0.01. *N* = 3.

fibroblasts, but poorly adherent to keratinocytes. In contrast, PVA-coated surface was almost nonadherent to all three cells tested and we could hardly detect DP cells, fibroblasts, and keratinocytes on PVA-coated glass at 6 h after seeding. The result here showed that PVA coating could serve as a barrier to prevent all three cells from adhering to the surface.

Time-Dependent Change in Cell-Substratum Adhesivity on PVA-Coated Glass and Serum Protein Adsorption. We speculated that if the nonadherent surface of PVA could progressively become adherent to cells in culture, the barrier effect would spontaneously diminish and cells seeded later could adhere to the originally nonadherent area. We tested whether PVA had this biphasic change in cell adhesivity. We incubated PVA-coated glass in fresh culture medium containing 10% FBS in DMEM for 1 to 4 days before cell seeding. We found that the adhesivity of both fibroblasts and DP cells on PVA-coated glass gradually increased after exposure to culture medium for 1 to 3 days and then the adhesivity plateaued (Figures 3A and 3B).

It has been shown that protein adsorption affected substratum adhesivity to cells.³³ Consistent with the progressive increase of cell-substratum adhesivity, we also found a corresponding trend of increasing protein adsorption to the PVA-coated surface from day 1 to day 3 (Figure 3C).

On the contrary, there were no significant differences of adhesivity to fibroblasts of uncoated glass after they were pre-exposed to culture medium for 1 to 4 days (Figure 3D). We also found that the protein adsorbed to uncoated glass showed no significant change as the duration of exposure to culture medium was increased (Figure 3E). Compared with PVA-coated glass, uncoated glass adsorbed serum proteins faster. PVA-coated glass showed a slow but progressively increased adsorption of serum proteins. The result suggested that the slow but progressive increase of protein adsorption on PVA from day 1 to day 3 may contribute to the progressive increase in cell adhesivity.

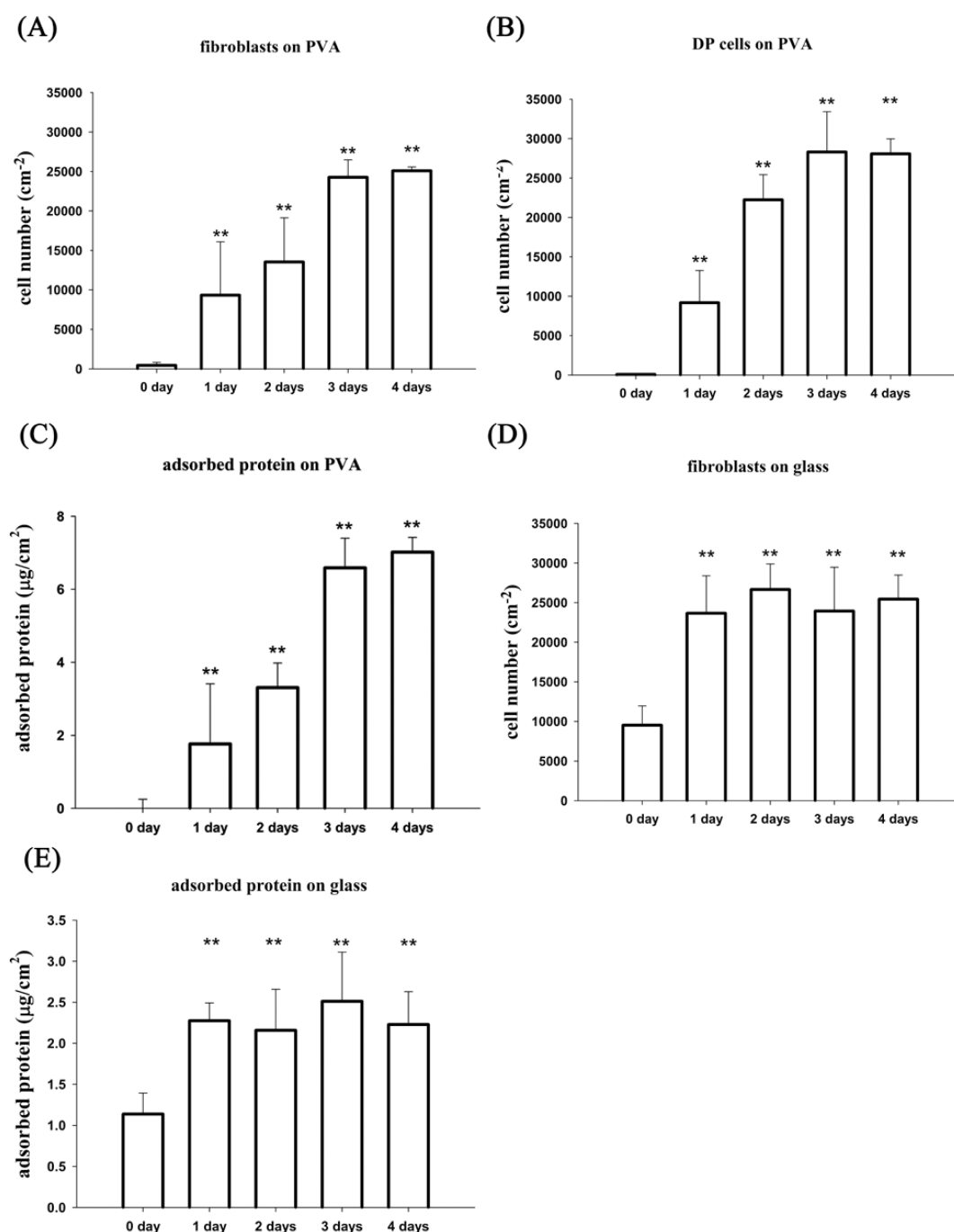


Figure 3. Time-dependent changes of substratum adhesivity and serum protein adsorption. (A) Adhesivity of fibroblasts on PVA. (B) Adhesivity of DP on PVA. (C) Serum protein adsorption of PVA. (D) Adhesivity of fibroblasts on glass. (E) Serum protein adsorption of glass. Asterisk denotes significant difference from 0 day group; * $p < 0.05$, ** $p < 0.01$. $N = 3$.

Adjustable Fast Design of Surface Topology for Cell Patterning with Programmable CO₂ Laser Ablation. We have shown that a programmable CO₂ laser system could fabricate complex surface topology on glass.¹⁹ With PVA as the barrier to cell adhesion, we could selectively create areas for cell adhesion by removing PVA through laser ablation. We and other group have shown that aggregation of DP cells into spheroids was vital to its function and hair follicle induction ability.^{29,30,34,35} Thus, we tested whether we could create arrays of microwells on the glass surface for DP cells to adhere to. Programmable laser ablation allowed us to create arrays of

microwells on the PVA-coated glass chip with controllable microwell sizes and spacing (Figure 4A).

It has been shown that the shorter edge-to-edge distance (D) (the edge of one microwell to the neighboring one) could lead to formation of cell bridge between microwells.²⁸ To determine the minimal edge-to-edge distance that could prevent cell bridge formation, we varied the D of microwells for the culture of DP cells. We found that at the D of 200 μm , cell bridges formed (Figure 4B). As D was increased to 450 and 750 μm , DP cells formed isolated aggregates in the microwells without cell bridge formation (Figure 4B). The result suggested that D

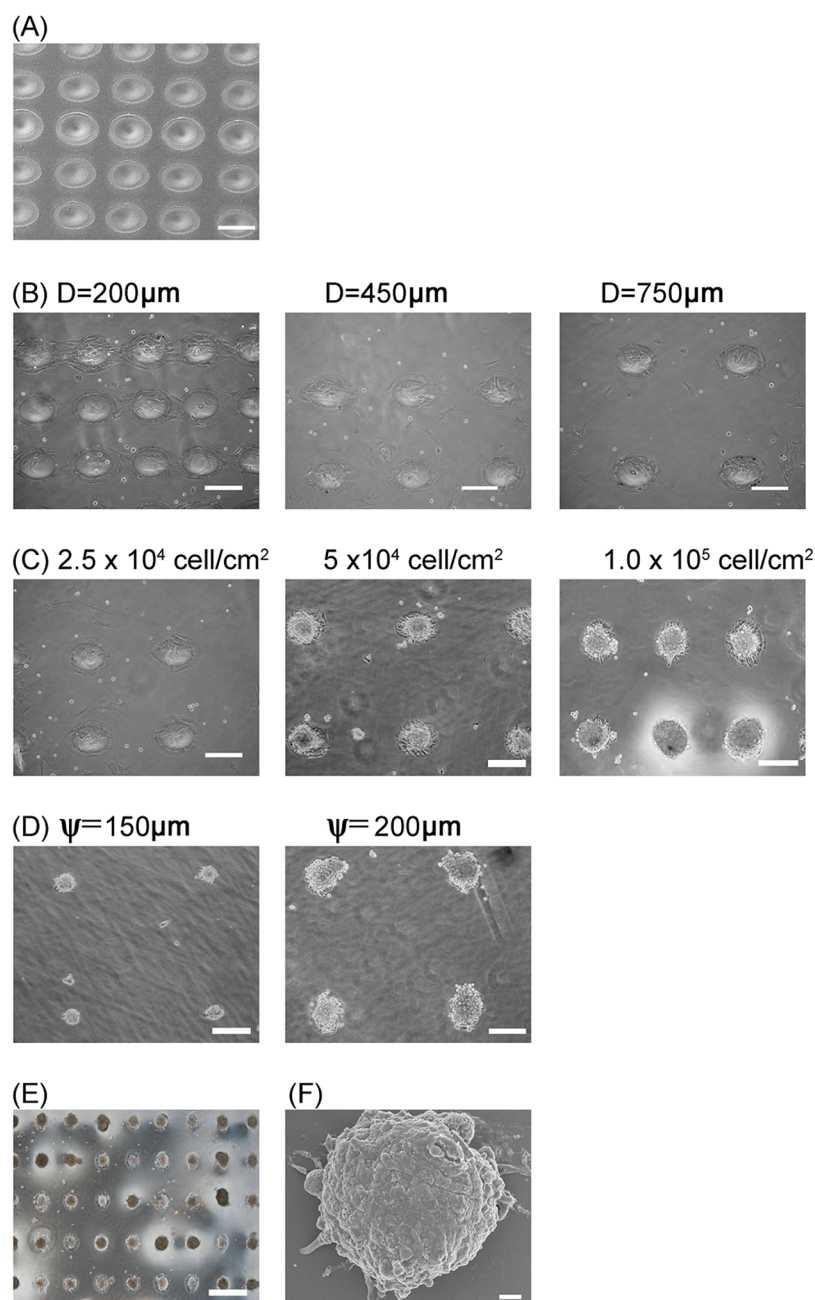


Figure 4. (A) Phase contrast image showed arrays of microwells on glass surface. (B) Microwells of different intermicrowell distances for DP cell culture. Phase contrast image. (C) Variation of seeding densities of DP cells. Phase contrast image. (D) Variation of microwell diameters for DP cell culture. Phase contrast image. (E) Phase contrast of arrays of spheroidal DP cell aggregates and (F) scanning electron micrograph of a spheroidal DP cell aggregates formed under the condition: $D = 300 \mu\text{m}$, $\psi = 200 \mu\text{m}$, DP cell seeding density $1.0 \times 10^5/\text{cm}^2$. Scale bar: $200 \mu\text{m}$ in A–D, $500 \mu\text{m}$ in E, $10 \mu\text{m}$ in F.

larger than $200 \mu\text{m}$ could help to create isolated islands of DP aggregates.

We then tested the effect of cell seeding density on cell aggregation in the microwells. We found DP cells started to form spheroidal aggregates in the microwells as the cell seeding density was increased to $2.5 \times 10^4/\text{cm}^2$ (Figure 4C). With serial increase of the cell seeding density, the morphology of the attached DP cells gradually change from a flat morphology to spheroidal aggregates in the microwells (Figure 4C).

Furthermore, to clarify the effect of sizes of microwells on cell aggregate formation, DP cells were seeded on the glass chip with various microwell sizes (ψ) at the same cell seeding

density. The size of DP cell aggregates could be regulated by the size of microwells (Figure 4D).

The results above showed that microwell size, intermicrowell distance and cell seeding density affected the final morphology and patterns of seeded DP cells in culture. We used the condition ($D = 300 \mu\text{m}$, $\psi = 200 \mu\text{m}$, DP cell seeding density $1.0 \times 10^5/\text{cm}^2$) for following experiments. Under this condition, arrays of spheroidal DP cell aggregates could be obtained (Figures 4E and 4F).

Creation of Patterns Involving 3 Heterotypic Cells. We then tested whether we could pattern DP cells and fibroblasts into islands of DP aggregates in a background of fibroblast

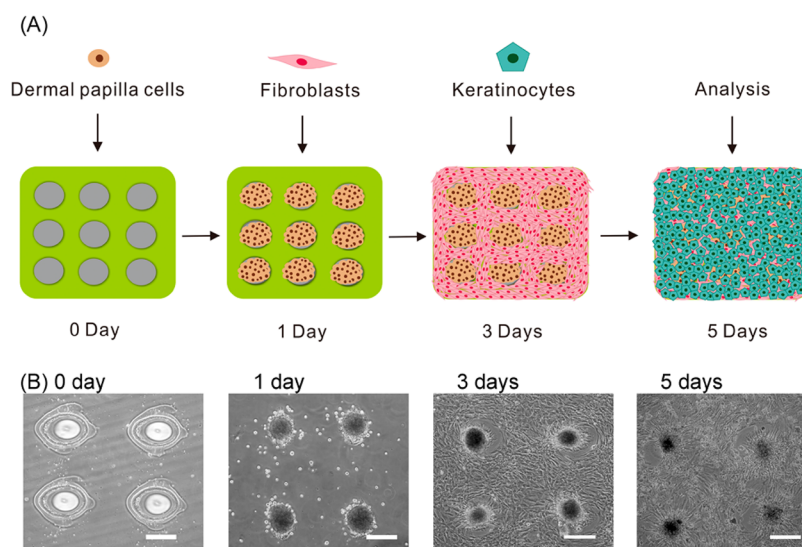


Figure 5. (A) Sequential seeding of DP cells, fibroblasts and keratinocytes. (B) Phase-contrast images of cell morphology on laser ablated PVA-coated glass by sequential cell seeding. Bar: 200 μm .

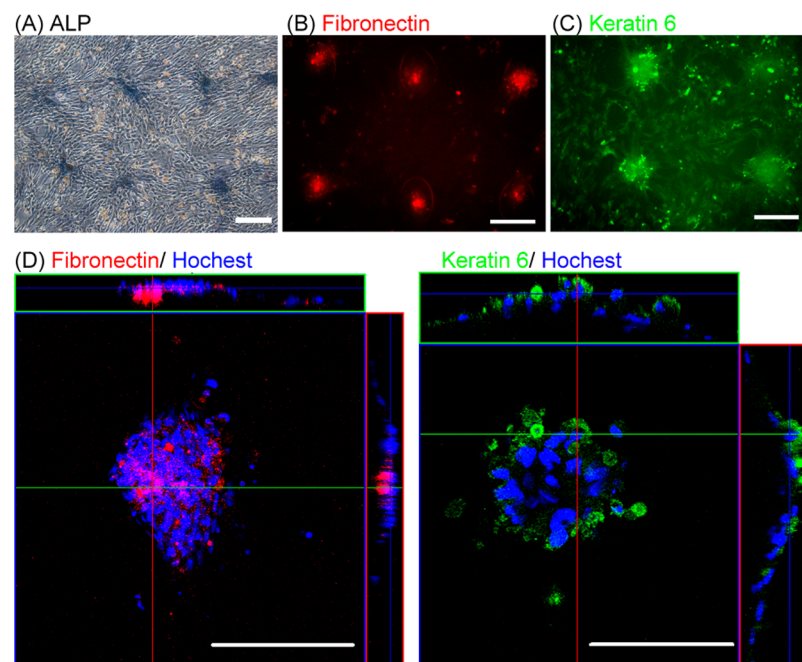


Figure 6. Characterization of hybrid microtissues in the microwells after 5 days in culture. (A) ALP activity, (B) fibronectin, and (C) keratin 6 expressions. (D) Confocal image of fibronectin and keratin 6 expression of the hybrid microtissue in the microwells. Fibronectin was present in DP cell aggregates, while keratin 6 was expressed by keratinocytes on top of DP cells. Bar = 200 μm .

sheet by sequential cell seeding. DP cells were first seeded on to the glass at the density of $1.0 \times 10^5/\text{cm}^2$. After 1 day in culture, we could see aggregated DP spheroid on islands of microwells (Figure 5). We then removed the nonadherent DP cells suspended in the medium and fibroblasts were seeded. After another 2 days in culture, we found fibroblasts attached and formed a cell sheet around islands of DP spheroids (Figure 5). Hence, sequential seeding of DP cells and fibroblasts could pattern these two types of cells into arrays of DP spheroids surrounded by a fibroblast sheet. Keratinocytes were then seeded subsequently on day 3.

Keratinocytes usually adhere poorly to culture surface. We previously showed that mesenchymal cells, such as DP cells, showed higher adhesivity to keratinocytes than culture surface

and could help to pull the keratinocytes down to the culture surface.²⁸ After another 2 days in culture following the seeding of the keratinocytes, we found that keratinocytes could adhere to the surface with patterned distribution of DP cells and fibroblasts (Figure 5).

Heterotypic Intercellular Interaction. We then characterize functions of the patterned three heterotypic cells by examining the expression of alkaline phosphatase, fibronectin, and keratin 6. It has been shown that alkaline phosphatase activity and enriched fibronectin in vitro correlated with the hair follicle induction of DP cells. Our result showed that alkaline phosphatase activity and expression of fibronectin were preferentially located in the DP aggregates in the microwells (Figures 6A, 6B, and 6D), suggesting that DP cells retained

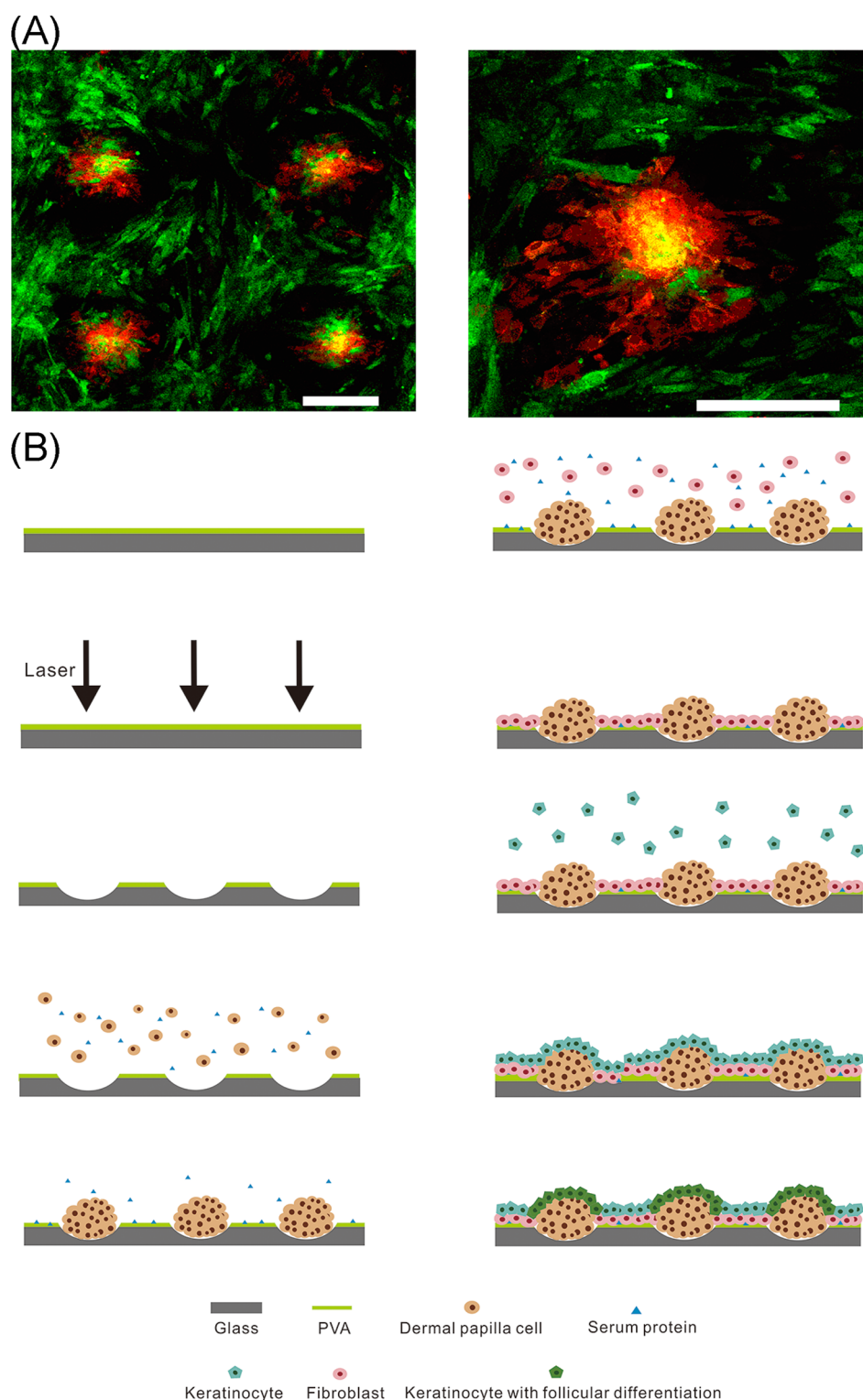


Figure 7. (A) Confocal images of the patterned sequentially seeded fibroblasts. Rat fibroblasts with orange cell tracker was seeded on day 0, and 3T3 fibroblasts with green cell tracker was seeded on day 1. The confocal fluorescent images were taken on day 4. Fibroblasts seeding density was $5 \times 10^4/\text{cm}^2$. Bar: $200 \mu\text{m}$. (B) Summary of PVA-coating, laser microfabrication and sequential cell seeding to pattern DP cells, fibroblasts, and keratinocytes for compartmented epithelial–mesenchymal interaction on a glass chip.

their differentiation status and hair follicle induction ability here. On the contrary, fibroblasts surrounding DP islands were deficient in alkaline phosphatase activity.

DP cells have been shown to be able to induce follicular differentiation of keratinocytes. We examined the expression of keratin 6, a differentiation marker of hair follicle outer root

sheath cells.³⁶ Keratinocytes contacting DP aggregates showed a strong staining for keratin 6 (Figure 6C), suggesting that epidermal keratinocytes here differentiated toward a follicular fate. Consistent with the results above, confocal images showed that the fibronectin expression was in the cell aggregate and the keratin 6 was expressed on top and at the periphery of the DP

aggregate (Figure 6D). The results here showed that we could pattern 3 heterotypic cells into desired intercellular arrangement to control heterotypic epithelial-mesenchymal interaction.

Application to the Patterning of Other Cells. We also tested whether the arrangement of other mesenchymal cells could be patterned with this approach. Rat fibroblasts and 3T3 fibroblasts were seeded sequentially 1 day apart on laser-ablated PVA-coated glass. The first seeded rat fibroblasts also formed cell aggregates in the microwells while 3T3 fibroblasts preferentially attached to the unablated surface surrounding rat fibroblast aggregates (Figure 7A). The results suggested that the two kinds of mesenchymal cells could be patterned by this method.

DISCUSSION

Hair follicles are a miniorgan composed of epithelial keratinocytes and its unique mesenchymal cells of DP.³ Hair follicles exhibit distinct cycles of growth (anagen), regression (catagen) and resting (telogen) in life. The development and cycling are dependent on the complicated epithelial-mesenchymal interaction between keratinocytes and DP.^{2,3} Up to date, the epithelial-mesenchymal interaction of hair follicles, i.e. interaction between hair follicle epithelium and DP cells, can only be investigated by transwells and organ culture of hair follicles.^{8,37} It has been shown that the heterotypic cell-cell contact between hair follicle epithelium and DP is also vital to maintenance of proper hair follicle growth.^{34,35,38} Transwell culture prohibited heterotypic epithelial-mesenchymal cell contact and may not reflect the in vivo heterotypic cell-cell interaction. Through hair follicle organ culture maintains the proper epithelial-mesenchymal contact, the limited sources of human follicles hinder scalable in vitro testing.

Methods for controllable patterned epithelial-mesenchymal interaction of skin cells on a chip have not been developed. Considering the simultaneous seeding of the three types of cells, DP cells, fibroblasts and keratinocytes, there are many possibilities of the final intercellular organizations formed on the same surface (Figure S1). Usually, for cell patterning, substratum surface was often modified by photolithography or soft lithography involving complex chemical, physical or phase transition process.^{21,39,40} Here we demonstrated a simple method capable of patterning heterotypic cutaneous mesenchymal cells on a glass chip with time-switchable coating (PVA) and CO₂ laser microfabrication with sequential cell seeding.

The dynamic changes of intercellular rearrangement are depicted in (Figure 7B). This method enabled creation of tissue-like structure composed of arrays of DP cell aggregates of controllable size distributed on a background of fibroblasts covered with keratinocytes above. DP cells first attached and aggregated in the microwells, forming arrays of DP spheroids within 24 h. The later seeded fibroblasts preferentially adhered to the PVA domains and grew as a flat cell sheet. The finally seeded keratinocytes were sorted to the surface contacting the DP aggregates and fibroblast sheet. Further testing showed that that controllable epithelial-mesenchymal contact and interaction was achieved (Figure 6).

It was shown that prepatterned compartmented distribution of epithelial cells and mesenchymal cells within an organ germ in vitro can facilitate epithelial-mesenchymal interaction than random mixture of epithelial cells and mesenchymal cells.^{28,41,42} Our results showed that aggregated DP cells in the arrays of microwells induced local follicular differentiation of keratinocytes (Figure 6). We demonstrated this method is also able to

pattern other mesenchymal cells with similar properties. 3T3 fibroblasts and rat fibroblasts can be similarly patterned as DP cells and fibroblasts (Figure 7A).

We have previously developed a method to produce DP-keratinocyte hybrid spheroidal microtissues with a core-shell structure through self-assembly: aggregated DP cells in the center surrounded by keratinocytes, a structure similar to the hair bulb.²⁸ We have shown that reconstruction of epithelial-mesenchymal contact in the hybrid spheroid promotes the hair follicle differentiation of keratinocytes and the hybrid spheroids are capable of growing new hair follicles after in vivo transplantation.²⁸ Because the hybrid spheroids are floating in the medium, it has been difficult for serial analysis of the epithelial-mesenchymal interaction at the same microtissue. The method developed here allowed continuous observation of the epithelial-mesenchymal interaction at the same area. For example, the cells can be tagged with fluorescent reporters or fluorescent protein reporters and the epithelial-mesenchymal interaction can be continuously and noninvasively monitored under a fluorescent microscope. Since fibroblasts, DP cells and epithelial keratinocytes can be expanded before cell seeding, compared with organ culture of hair follicles, this method allowed large-scale pharmaceutical testing of epithelial-mesenchymal interaction.

One key component of this method is the unique property of PVA both as a barrier to cell adhesion in the early stage and a surface for cell attachment in the later stage. PVA is an extremely hydrophilic biomaterial,^{30,43} and has been used for the culture of a variety of cells.^{30,43-45} We and other group have shown that surface coating with PVA prevents the attachment of a variety of cells and promotes aggregation of unattached cells into floating spheroids. Here we uncovered another property of PVA. Though it is nonadherent to cells on the first day of cell culture, its adhesivity to fibroblasts and DP cells increased progressively as the exposure time to serum-containing culture medium is increased. The adhesivity of cells on biomaterial is determined both by the intrinsic property of biomaterial and the protein adsorbed.³³ Factors influencing protein adsorption include wettability of biomaterials, charge or chemical bond of biomaterial, pH, temperature, protein types, concentration of bulk solution, etc.^{46,47}

Compared with poly(ethylene), poly(vinyl alcohol-co-ethylene), and glass, hydrophilic surface of PVA film is a polymer on which serum proteins can be hardly absorbed.⁴⁸ Pavli et al. showed that PVA-covered surface could significantly prevent protein adsorption and there was only little amount of protein adsorbed on PVA surface after 22 h incubation.⁴⁹ From our present work (Figures 2 and 3), after 24 h of incubation, the increase of cell adhesivity on PVA correlated with the increase of protein adhesion on PVA. In addition, according to Hung's report,⁵⁰ soluble serum proteins deposited on PVA substratum could also improve cellular adhesion on PVA when cells were cultured in serum-free medium. Thus, we suggest that the increased cell adhesivity after 24 h could be explained at least in part by the increase of proteins adsorbed on the PVA surface. Furthermore, due to the complex compositions of serum proteins, including fibronectin, fibrinogen, albumin, etc., the conformations of adsorbed proteins might also be influenced by other proteins in serum.⁵¹ For example, fibronectin is one of the well-known extracellular matrix proteins in serum that can promote cell adhesion. Previous computer simulation showed that, due to the hydrogen bond and dipolar interaction between the chain of PVA and proteins, the serum albumin and

fibronectin might form α -helices and β -sheets on PVA individually.⁵² Moreover, the conformations of plasma fibronectin could be changed by the hydrophobicity of the surface. When adsorbed on hydrophilic substrate, fibronectin might adopt an active cell-spreading and antigen active conformation.⁵³ Therefore, the increase of cell-adhesivity after 24 h might also be contributed by the conformations of the serum proteins adsorbed on PVA.⁵⁴

According to the molecular mean-field theory, serum proteins diffuse from solution to the PVA surface and then form a Van der Waals force or hydrogen bond to overcome entropy and Gibbs free energy of material interface to deposit on the PVA surface.^{55,56} In our system, compared with PVA, glass is more hydrophobic than PVA;⁵⁷ there is less energy barrier of dehydration needed to be overcome so that DP cell could adhere on ablated area within 24 h. With the time of incubation in serum-containing medium increased, more serum proteins started to deposit on PVA surface via the hydrophilic fragment of serum proteins attracted by hydroxyl group of PVA, the energy of PVA surface could be changed and overcome the dehydration energy barrier. Then, fibroblasts could adhere on protein-adsorbed PVA surface after 24 h. Therefore, this can be a mechanism why cell adhesion is increased after the amount of adsorbed protein is increased. In terms of adsorption dynamics, our results showed that protein adsorption on PVA surface gradually increased, following a time-dependent manner in serum-containing culture medium. It is consistent with molecular mean-field theory in which protein adsorption is a time-dependent dynamic process.^{55,56} The relative slow protein adsorption gives us a window in which the first seeded cells are unable to attach to the PVA-coated surface and preferentially adhere and aggregate into the CO₂ laser ablated microwells (Figure 7B). After 24 h, the increase in adhesivity allows the adherence of fibroblasts. The patterned DP cell and fibroblast distribution enables us to examine epithelial-mesenchymal interaction of three different types of cells (Figure 7B).

The use of CO₂ laser provides other advantages. Since the laser parameters can be programmed,^{19,58} the surface topology of the culture surface can be flexibly fabricated while PVA being removed at the same time. We have demonstrated that CO₂ laser ablation is able to create complex topological structures on the glass and plastics surfaces.^{58,59} Since the DP function is better preserved as multicellular aggregates, we employed CO₂ laser to create arrays of microwells such that DP cells formed spheroidal microtissues after seeding (Figure 4). With such flexibility, this method is versatile in topological manipulation. Alternatively, lasers other than CO₂ laser can also be used in this system provided that an alternative laser source can efficiently remove the coated PVA and fabricate the surface topology.^{20,59,60}

Additionally, PVA can be replaced by other biomaterials or proteins with desired properties for surface coating. This will further increase the patterning possibilities. The order of surface coating and laser ablation can also be changed and each treatment can be repeated, this again will increase the freedom of cell patterning and cells can be patterned in diverse ways.

CONCLUSION

We successfully develop a method for heterotypic cell patterning with flexible topological fabrication capability by combining PVA-coating, CO₂ laser ablation and sequential cell seeding on a glass chip. This method utilizes a characteristic

property of PVA that shows biphasic change in cell adhesivity associated with delayed serum adsorption. We show that this method is able to create arrays of DP aggregates surrounded by a fibroblast sheet and that controllable epithelial-mesenchymal interaction can be achieved. We also show that mesenchymal cells with similar properties can also be patterned on the glass chip. This method can be helpful for large-scale investigation and pharmaceutical testing of cutaneous epithelial-mesenchymal interaction and can also be applied to the patterning of other cells.

ASSOCIATED CONTENT

Supporting Information

The Supporting Information is available free of charge on the ACS Publications website at DOI: 10.1021/acsami.5b05978.

Examples of possible patterns of intercellular organization after seeding of 3 types of cells on a biomaterial substratum (PDF)

AUTHOR INFORMATION

Corresponding Author

*Tel: +886-2-23562141. Fax: +886-2-23934177. E-mail: drsjlin@ntu.edu.tw.

Author Contributions

#Y.-C. Li and M.-W. Lin contributed equally to this work.

Notes

The authors declare no competing financial interest.

ACKNOWLEDGMENTS

This work was supported by grants from Taiwan Ministry of Science and Technology (99-2320-B-002-004-MY3, 103-2325-B-002-008, 103-2628-B-002-004-MY3), National Taiwan University Hospital (104-S2707, VN104-12), and Taiwan National Health Research Institutes (NHRI-EX104-10401EI).

REFERENCES

- (1) Lin, S. J.; Foley, J.; Jiang, T. X.; Yeh, C. Y.; Wu, P.; Foley, A.; Yen, C. M.; Huang, Y. C.; Cheng, H. C.; Chen, C. F.; Reeder, B.; Jee, S. H.; Widelitz, R. B.; Chuong, C. M. Topology of Feather Melanocyte Progenitor Niche Allows Complex Pigment Patterns to Emerge. *Science* **2013**, *340* (6139), 1442–1445.
- (2) Millar, S. E. Molecular Mechanisms Regulating Hair Follicle Development. *J. Invest. Dermatol.* **2002**, *118* (2), 216–225.
- (3) Schneider, M. R.; Schmidt-Ullrich, R.; Paus, R. The Hair Follicle as A Dynamic Miniorgan. *Curr. Biol.* **2009**, *19* (3), R132–142.
- (4) Turing, A. M. The Chemical Basis of Morphogenesis. *Philos. Trans. R. Soc., B* **1952**, *237* (641), 37–72.
- (5) Crick, F. Diffusion in Embryogenesis. *Nature* **1970**, *225* (5231), 420.
- (6) Vestweber, D. Cadherins in Tissue Architecture and Disease. *J. Mol. Med.* **2015**, *93* (1), 5–11.
- (7) Bhatia, S. N.; Balis, U. J.; Yarmush, M. L.; Toner, M. Effect of Cell-Cell Interactions in Preservation of Cellular Phenotype: Cocultivation of Hepatocytes and Nonparenchymal Cells. *FASEB J.* **1999**, *13* (14), 1883–1900.
- (8) Sheen, Y. S.; Fan, S. M.; Chan, C. C.; Wu, Y. F.; Jee, S. H.; Lin, S. J. Visible Red Light Enhances Physiological Anagen Entry in Vivo and Has Direct and Indirect Stimulative Effects in Vitro. *Lasers Surg. Med.* **2015**, *47* (1), 50–59.
- (9) Inui, S.; Fukuzato, Y.; Nakajima, T.; Yoshikawa, K.; Itami, S. Androgen-inducible TGF- β 1 from Balding Dermal Papilla Cells Inhibits Epithelial Cell Growth: a Clue to Understand Paradoxical Effects of Androgen on Human Hair Growth. *FASEB J.* **2002**, *16* (14), 1967–1969.

- (10) Chan, C. C.; Fan, M. Y.; Wang, W. H.; Mu, Y. F.; Lin, S. J. A Two-stepped Culture Method for Efficient Production of Trichogenic Keratinocytes. *Tissue Eng, Part C* **2015**, 150612131326002.
- (11) Verhulsel, M.; Vignes, M.; Descroix, S.; Malaquin, L.; Vignjevic, D. M.; Viovy, J. L. A Review of Microfabrication and Hydrogel Engineering for Micro-organs on Chips. *Biomaterials* **2014**, 35 (6), 1816–1832.
- (12) Bhatia, S. N.; Yarmush, M. L.; Toner, M. Controlling Cell Interactions by Micropatterning in Co-cultures: Hepatocytes and 3T3 Fibroblasts. *J. Biomed. Mater. Res.* **1997**, 34 (2), 189–199.
- (13) Chiu, D. T.; Jeon, N. L.; Huang, S.; Kane, R. S.; Wargo, C. J.; Choi, I. S.; Ingber, D. E.; Whitesides, G. M. Patterned Deposition of Cells and Proteins onto Surfaces by Using Three-dimensional Microfluidic Systems. *Proc. Natl. Acad. Sci. U. S. A.* **2000**, 97 (6), 2408–2413.
- (14) Poujade, M.; Grasland-Mongrain, E.; Hertzog, A.; Jouanneau, J.; Chavier, P.; Ladoux, B.; Buguin, A.; Silberzan, P. Collective Migration of An Epithelial Monolayer in Response to a Model Wound. *Proc. Natl. Acad. Sci. U. S. A.* **2007**, 104 (41), 15988–15993.
- (15) Qin, D.; Xia, Y.; Whitesides, G. M. Soft Lithography for Micro- and Nanoscale Patterning. *Nat. Protoc.* **2010**, 5 (3), 491–502.
- (16) Folch, A.; Jo, B. H.; Hurtado, O.; Beebe, D. J.; Toner, M. Microfabricated Elastomeric Stencils for Micropatterning Cell Cultures. *J. Biomed. Mater. Res.* **2000**, 52 (2), 346–353.
- (17) Guillotin, B.; Souquet, A.; Catros, S.; Duocastella, M.; Pippenger, B.; Bellance, S.; Bareille, R.; Remy, M.; Bordenave, L.; Amedee, J.; Guillemot, F. Laser Assisted Bioprinting of Engineered Tissue with High Cell Density and Microscale Organization. *Biomaterials* **2010**, 31 (28), 7250–7256.
- (18) Falconnet, D.; Csucs, G.; Grandin, H. M.; Textor, M. Surface Engineering Approaches to Micropattern Surfaces for Cell-based Assays. *Biomaterials* **2006**, 27 (16), 3044–3063.
- (19) Yen, M. H.; Cheng, J. Y.; Wei, C. W.; Chuang, Y. C.; Young, T. H. Rapid Cell-patterning and Microfluidic Chip Fabrication by Crack-free CO₂ Laser Ablation on Glass. *J. Micromech. Microeng.* **2006**, 16 (7), 1143–1153.
- (20) Cheng, J. Y.; Yen, M. H.; Wei, C. W.; Chuang, Y. C.; Young, T. H. Crack-free Direct-writing on Glass Using a Low-power UV Laser in The Manufacture of a Microfluidic chip. *J. Micromech. Microeng.* **2005**, 15 (6), 1147–1156.
- (21) Lim, D.; Kamotani, Y.; Cho, B.; Mazumder, J.; Takayama, S. Fabrication of Microfluidic Mixers and Artificial Vasculatures Using a High-brightness Diode-pumped Nd: YAG Laser Direct Write Method. *Lab Chip* **2003**, 3 (4), 318–323.
- (22) Ihlemann, J.; Wolff, B.; Simon, P. Nanosecond and Femto-second Excimer Laser Ablation of Fused-Silica. *Appl. Phys. A: Solids Surf.* **1992**, 54 (4), 363–368.
- (23) Li, Y.; Itoh, K.; Watanabe, W.; Yamada, K.; Kuroda, D.; Nishii, J.; Jiang, Y. Y. Three-dimensional Hole Drilling of Silica Glass From The Rear Surface with Femtosecond Laser Pulses. *Opt. Lett.* **2001**, 26 (23), 1912–1914.
- (24) Klank, H.; Kutter, J. P.; Geschke, O. CO₂-laser Micromachining and Back-end Processing for Rapid Production of PMMA-based Microfluidic Systems. *Lab Chip* **2002**, 2 (4), 242–246.
- (25) Pelham, R. J.; Wang, Y. L. Cell Locomotion and Focal Adhesions are Regulated by Substrate Flexibility. *Proc. Natl. Acad. Sci. U. S. A.* **1997**, 94 (25), 13661–13665.
- (26) Engler, A. J.; Griffin, M. A.; Sen, S.; Bonnetmann, C. G.; Sweeney, H. L.; Discher, D. E. Myotubes Differentiate Optimally on Substrates with Tissue-like Stiffness: Pathological Implications for Soft or Stiff Microenvironments. *J. Cell Biol.* **2004**, 166 (6), 877–887.
- (27) Li, Y. C.; Liao, Y. T.; Chang, H. H.; Young, T. H. Covalent Bonding of GYIGSR to EVAL Membrane Surface to Improve Migration and Adhesion of Cultured Neural Stem/Precursor cells. *Colloids Surf., B* **2013**, 102, 53–62.
- (28) Yen, C. M.; Chan, C. C.; Lin, S. J. High-throughput Reconstitution of Epithelial-mesenchymal Interaction in Folliculoid Microtissues by Biomaterial-facilitated Self-assembly of Dissociated Heterotypic Adult Cells. *Biomaterials* **2010**, 31 (15), 4341–4352.
- (29) Young, T. H.; Lee, C. Y.; Chiu, H. C.; Hsu, C. J.; Lin, S. J. Self-assembly of Dermal Papilla Cells into Inductive Spheroidal Microtissues on Poly(ethylene-co-vinyl alcohol) Membranes for Hair Follicle Regeneration. *Biomaterials* **2008**, 29 (26), 3521–3530.
- (30) Huang, Y. C.; Chan, C. C.; Lin, W. T.; Chiu, H. Y.; Tsai, R. Y.; Tsai, T. H.; Chan, J. Y.; Lin, S. J. Scalable Production of Controllable Dermal Papilla Spheroids on PVA Surfaces and the Effects of Spheroid Size on Hair Follicle Regeneration. *Biomaterials* **2013**, 34 (2), 442–451.
- (31) Young, T. H.; Hu, W. W. Covalent Bonding of Lysine to EVAL Membrane Surface to Improve Survival of Cultured Cerebellar Granule Neurons. *Biomaterials* **2003**, 24 (8), 1477–1486.
- (32) Lin, S. J.; Jee, S. H.; Hsiao, W. C.; Lee, S. J.; Young, T. H. Formation of Melanocyte Spheroids on the Chitosan-Coated Surface. *Biomaterials* **2005**, 26 (12), 1413–1422.
- (33) Wyre, R. M.; Downes, S. The Role of Protein Adsorption on Chondrocyte Adhesion to a Heterocyclic Methacrylate Polymer System. *Biomaterials* **2002**, 23 (2), 357–364.
- (34) Reynolds, A. J.; Jahoda, C. A. B. Cultured Dermal Papilla Cells Induce Follicle Formation and Hair-Growth by Transdifferentiation of an Adult Epidermis. *Development* **1992**, 115 (2), 587–593.
- (35) Osada, A.; Iwabuchi, T.; Kishimoto, J.; Hamazaki, T. S.; Okochi, H. Long-term Culture of Mouse Vibrissal Dermal Papilla Cells and De Novo Hair Follicle Induction. *Tissue Eng.* **2007**, 13 (5), 975–982.
- (36) Moll, R.; Divo, M.; Langbein, L. The Human Keratins: Biology and Pathology. *Histochem. Cell Biol.* **2008**, 129 (6), 705–733.
- (37) Philpott, M. P.; Green, M. R.; Kealey, T. Human Hair Growth in Vitro. *J. Cell Sci.* **1990**, 97, 463–471.
- (38) McElwee, K. J.; Kissling, S.; Wenzel, E.; Huth, A.; Hoffmann, R. Cultured Peribulbar Dermal Sheath Cells can Induce Hair Follicle Development and Contribute to The Dermal Sheath and Dermal Papilla. *J. Invest. Dermatol.* **2003**, 121 (6), 1267–1275.
- (39) Schmid, H.; Michel, B. Siloxane Polymers for High-resolution, High-accuracy Soft Lithography. *Macromolecules* **2000**, 33 (8), 3042–3049.
- (40) Folch, A.; Jo, B. H.; Hurtado, O.; Beebe, D. J.; Toner, M. Microfabricated Elastomeric Stencils for Micropatterning Cell Cultures. *J. Biomed. Mater. Res.* **2000**, 52 (2), 346–353.
- (41) Honda, M. J.; Tsuchiya, S.; Sumita, Y.; Sagara, H.; Ueda, M. The Sequential Seeding of Epithelial and Mesenchymal Cells for Tissue-engineered Tooth Regeneration. *Biomaterials* **2007**, 28 (4), 680–689.
- (42) Lee, L. F.; Chuong, C. M. Building Complex Tissues: High-Throughput Screening for Molecules Required in Hair Engineering. *J. Invest. Dermatol.* **2009**, 129 (4), 815–817.
- (43) Young, T. H.; Hung, C. H. Change in Electrophoretic Mobility of PC12 Cells after Culturing on PVA Membranes Modified with Different Diamines. *J. Biomed. Mater. Res.* **2003**, 67 (4), 1238–1244.
- (44) Chen, R. S.; Chen, M. H.; Young, T. H. Induction of Differentiation and Mineralization in Rat Tooth Germ Cells on PVA through Inhibition of ERK1/2. *Biomaterials* **2009**, 30 (4), 541–547.
- (45) Kim, T. H.; An, D. B.; Oh, S. H.; Kang, M. K.; Song, H. H.; Lee, J. H. Creating Stiffness Gradient Polyvinyl Alcohol Hydrogel Using a Simple Gradual Freezing-thawing Method to Investigate Stem Cell Differentiation Behaviors. *Biomaterials* **2015**, 40, 51–60.
- (46) Andrade, J. D.; Hlady, V.; Wei, A. P. Adsorption of Complex Proteins at Interfaces. *Pure Appl. Chem.* **1992**, 64 (11), 1777–1781.
- (47) Wilson, C. J.; Clegg, R. E.; Leavesley, D. I.; Percy, M. J. Mediation of Biomaterial-cell Interactions by Adsorbed Proteins: A review. *Tissue Eng.* **2005**, 11 (1–2), 1–18.
- (48) Ikada, Y.; Iwata, H.; Horii, F.; Matsunaga, T.; Taniguchi, M.; Suzuki, M.; Taki, W.; Yamagata, S.; Yonekawa, Y.; Handa, H. Blood Compatibility of Hydrophilic Polymers. *J. Biomed. Mater. Res.* **1981**, 15 (5), 697–718.
- (49) Pavli, P.; Petrou, P. S.; Douvas, A. M.; Dimotikali, D.; Kakabakos, S. E.; Argitis, P. Protein-resistant Cross-linked Poly(vinyl alcohol) Micropatterns via Photolithography Using Removable Polyoxometalate Photocatalyst. *ACS Appl. Mater. Interfaces* **2014**, 6 (20), 17463–17473.

(50) Hung, C. H.; Young, T. H. Differences in the Effect on Neural Stem Cells of Fetal Bovine Serum in Substrate-coated and Soluble form. *Biomaterials* **2006**, *27* (35), 5901–5908.

(51) Benni, S.; Avramoglou, T.; Hlawaty, H.; Mora, L. Dynamic Contact angle Analysis of Protein Adsorption on Polysaccharide Multilayer's Films for Biomaterial Reendothelialization. *BioMed Res. Int.* **2014**, *2014*, 679031.

(52) Raffaini, G.; Ganazzoli, F. Protein Adsorption on the Hydrophilic Surface of a Glassy Polymer: a Computer Simulation Study. *Phys. Chem. Chem. Phys.* **2006**, *8* (23), 2765–2772.

(53) Grinnell, F.; Feld, M. K. Fibronectin Adsorption on Hydrophilic and Hydrophobic Surfaces Detected by α Antibody Binding and Analyzed During Cell Adhesion in Serum-containing Medium. *J. Biol. Chem.* **1982**, *257* (9), 4888–4893.

(54) Krammer, A.; Lu, H.; Isralewitz, B.; Schulten, K.; Vogel, V. Forced Unfolding of the Fibronectin Type III Module Reveals a Tensile Molecular Recognition Switch. *Proc. Natl. Acad. Sci. U. S. A.* **1999**, *96* (4), 1351–1356.

(55) Sivaraman, B.; Fears, K. P.; Latour, R. A. Investigation of the Effects of Surface Chemistry and Solution Concentration on the Conformation of Adsorbed Proteins Using an Improved Circular Dichroism Method. *Langmuir* **2009**, *25* (5), 3050–3056.

(56) Fang, F.; Szleifer, I. Kinetics and Thermodynamics of Protein Adsorption: A Generalized Molecular Theoretical Approach. *Biophys. J.* **2001**, *80* (6), 2568–2589.

(57) Rohr, T.; Ogletree, D. F.; Svec, F.; Fréchet, J. M. J. Surface Functionalization of Thermoplastic Polymers for the Fabrication of Microfluidic Devices by Photoinitiated Grafting. *Adv. Funct. Mater.* **2003**, *13* (4), 264–270.

(58) Cheng, J. Y.; Wei, C. W.; Hsu, K. H.; Young, T. H. Direct-write Laser Micromachining and Universal Surface Modification of PMMA for Device Development. *Sens. Actuators, B* **2004**, *99* (1), 186–196.

(59) Cheng, J. Y.; Yen, M. H.; Young, T. H. Crack-free Micromachining on Glass Using an Economic Q-switched 532 nm Laser. *J. Micromech. Microeng.* **2006**, *16* (11), 2420–2424.

(60) Zimmer, K.; Braun, A.; Bohme, R. Etching of Fused Silica and Glass with Excimer Laser at 351 nm. *Appl. Surf. Sci.* **2003**, *208*, 199–204.